Am J Cancer Res 2025;15(11):4885-4904
www.ajcr.us /ISSN:2156-6976/ajcr0168238

Original Article

Role and mechanism of the CBX4-HDAC5-CERS6 axis in disrupting sphingomyelin metabolism in acute myeloid leukemia

Ruifang Ye[1,2], Mingwei Sun[3], Jixian Huang[4], Lei Sun[5], Yao Wu[2], Xiangli Zou[2], Huanwen Tang[6]

[1]Guangdong Medical University First School of Clinical Medicine, Zhanjiang, Guangdong, China; [2]Dongguan Key Laboratory of Environmental Medicine, The First Dongguan Affiliated Hospital, School of Public Health, Guangdong Medical University, Dongguan, Guangdong, China; [3]The Sixth People's Hospital of Dongguan, Dongguan, Guangdong, China; [4]Yuebei People's Hospital, Shaoguan, Guangdong, China; [5]Dongguan First Hospital Affiliated to Guangdong Medical University, Dongguan, Guangdong, China; [6]School of Public Health, The Affiliated Dongguan Occupational Disease Prevention and Control Hospital, Guangdong Medical University, Dongguan, Guangdong, China

Received August 20, 2025; Accepted November 9, 2025; Epub November 25, 2025; Published November 30, 2025

Abstract: Objective: To investigate the mechanism by which the CBX4-HDAC5-CERS6 axis regulates sphingolipid metabolism in acute myeloid leukemia (AML), with the goal of providing new theoretical foundations for the targeted therapy of AML. Methods: This prospective study involved 50 AML patients and 50 healthy controls. The expression levels of CBX4, CERS6, and free ceramide were detected. RNA sequencing, proteomics, and lipidomics were employed to analyze CBX4's regulatory effects on sphingolipid metabolism-related genes and pathways. Using THP-1 and KG-1 cell lines, we validated the molecular mechanisms of the CBX4-HDAC5-CERS6 axis through techniques including gene knockdown (siRNA), overexpression, chromatin immunoprecipitation (ChIP), and dual-luciferase reporter assays. CCK-8 assay, flow cytometry, and Western blot were used to analyze the effects of CBX4 on cell proliferation, cell cycle, and key signaling pathways. Results: CBX4 was significantly overexpressed in AML cells, with its expression levels markedly higher in THP-1 and KG-1 cell lines compared with $CD34^+$ normal hematopoietic stem cells ($P<0.05$). Analysis of clinical samples revealed that the mRNA expression levels of CBX4 and CERS6 as well as free ceramide content were significantly lower in the AML group than the control group (all $P<0.05$). Mechanistic studies demonstrated that CBX4 knockdown significantly downregulated both mRNA and protein expression of CERS6 ($P<0.05$) and activated the PI3K/AKT and MAPK signaling pathways. Furthermore, CBX4 indirectly regulated CERS6 transcription by suppressing HDAC5 expression, and dual-luciferase reporter assays confirmed that HDAC5 directly targets the CERS6 promoter region ($P<0.05$). Combined use of ceramide synthesis inhibitors synergistically enhanced the activation of p-AKT/p-PI3K and p-MEK1/2/p-Raf1 signaling pathway associated proteins induced by CBX4 knockdown. Conclusion: The CBX4-HDAC5-CERS6 axis influences AML malignant progression by regulating sphingolipid metabolism, and targeted intervention of this axis may represent a novel therapeutic strategy for AML.

Keywords: Acute myeloid leukemia, CBX4-HDAC5-CERS6 axis, sphingomyelin, mechanism

Introduction

Acute Myeloid Leukemia (AML) is a malignant tumor characterized by the abnormal proliferation of hematopoietic cells, primarily resulting from the clonal expansion of undifferentiated myeloid blast cells derived from aberrant hematopoietic stem cells (HSCs) [1]. The core manifestations of the disease involve blocked differentiation of normal hematopoietic stem cells coupled with dysregulated self-renewal of malignant hematopoietic stem cells [2]. Globally, approximately 120,000 new AML cases are diagnosed annually, with a mortality rate of around 30%. The overall prognosis remains poor, with a five-year survival rate of only 30%-35%, which significantly diminishes patients' quality of life and imposes a substantial healthcare burden [3]. Research indicates that the remodeling of lipid metabolic pathways is a sig-

https://doi.org/10.62347/VXBP2060

nificant contributor to the poor prognosis of AML [4].

Sphingolipid (SP) metabolism, a key part in lipid metabolism, plays critical roles in cellular adhesion, proliferation, migration, and death [5]. SP can be structurally classified into three categories: sphingosine-1-phosphate (S1P), ceramides, and complex SP, with ceramides serving as the central component of SP metabolism [6]. Ceramides initiate apoptotic pathways and induce cell death by activating mitochondrial permeability, which leads to the release of harmful substances into the cytosol, representing a key mechanism through which SP regulate apoptosis [7]. Ceramide, a homeostatic regulator of SP balance, plays a critical role in cancer metastasis through its dysregulated or abnormal expression [8].

In the regulatory network of SP metabolism, CBX4, HDAC5, and CERS6 play distinct yet closely interrelated roles [9]. CBX4, as a core component of the Polycomb Repressive Complex 1 (PRC1), exerts dual functions in epigenetic regulation and SUMO E3 ligase activity. By modulating histone modifications and transcription factor activity, CBX4 shapes gene expression profiles that subsequently regulate critical cellular processes including proliferation, differentiation, and inflammatory responses [10]. CBX4-mediated SUMOylation of HIF-1α plays a critical role in various pathological processes, including angiogenesis, atherosclerosis, and asthma [11]. This demonstrates that beyond its involvement in transcriptional regulation, CBX4 also modulates multiple signaling pathways through its SUMO E3 ligase activity, thereby influencing cellular functions associated with SP metabolism [12].

HDAC5, a Class IIa histone deacetylase, primarily catalyzes both histone and non-histone proteins, thereby modulating chromatin structure and gene transcription [13]. HDAC5 promotes tumor cell proliferation and metastasis by interacting with CBX4 to facilitate the transcriptional repression of tumor suppressor genes [14]. This finding not only suggests that HDAC5 is potentially regulated by CBX4, but also establishes HDAC5 as a key regulatory factor in SP metabolism and its associated diseases [14].

CERS6, a key enzyme in the SP synthesis pathway, primarily catalyzes the production of C16 acyl-chain ceramides. As central intermediates in sphingolipid metabolism, ceramides regulate crucial cellular processes including apoptosis, proliferation, and stress response [15]. CERS6-regulated accumulation of C16-ceramide is closely associated with mitochondrial dysfunction, aberrant apoptosis, and dysregulated autophagy, playing important roles in cerebral hemorrhage, neurodegenerative diseases, and immune regulation [16]. Research demonstrates that CBX4 can bind to the promoter region of the CERS6 gene and modulate its transcriptional activity, thereby influencing CERS6 expression levels. This mechanism enables cells to dynamically adjust CERS6 production according to metabolic demands, achieving precise regulation of SP synthesis [17]. On the other hand, HDAC5 modulates chromatin compaction at the CERS6 gene locus through its histone deacetylase activity, consequently influencing transcriptional efficiency. Such epigenetic alterations governed by HDAC5 can either suppress or activate CERS6 transcription, enabling cells to adapt SP synthesis according to varying physiological or pathological requirements [18]. These findings demonstrate that CERS6 serves not only as a key enzyme in SP synthesis - subject to regulation by both CBX4 and HDAC5 - but also plays a central role in diseases associated with aberrant SP metabolism.

In summary, CBX4, HDAC5, and CERS6 function coordinately at different levels of SP metabolism. CBX4 modulates SP-related genes and signaling pathways through epigenetic regulation and SUMOylation. HDAC5 fine-tunes gene expression and protein functions via its deacetylase activity. CERS6, as the key synthetic enzyme, directly controls ceramide production and accumulation. The functional interplay among these three components not only maintains SP metabolic homeostasis but also contributes to the pathogenesis of various diseases [18]. Elucidating the molecular mechanisms and regulatory networks governing CBX4, HDAC5, and CERS6 will advance our understanding of the complex regulatory mechanism underlying SP metabolism, potentially revealing novel therapeutic targets and diagnostic strategies for AML.

Material and methods

Patient population

This study prospectively enrolled patients with AML admitted to Yuebei People's Hospital between January and December 2022. The

diagnosis was based on the AML classification criteria issued by the European LeukemiaNet (ELN) and the National Comprehensive Cancer Network (NCCN) guidelines [19, 20]. After obtaining informed consent from the patients, bone marrow blood samples or bone marrow biopsy specimens were collected as the study group (AML, n=50), and peripheral blood from healthy patients was collected as the control group (Control, n=50). The study protocol was approved by the Ethics Committee of Yuebei People's Hospital (Approval No.: KY-2021-274). Inclusion criteria: (1) Meeting the diagnostic criteria for primary AML; (2) Provision of written informed consent. Exclusion criteria: (1) History of other malignant tumors; (2) Severe organ dysfunction or major comorbidities; (3) Refusal to participate.

Data acquisition

In terms of data acquisition, AML and normal sample information were obtained from the Bloodspot database (https://servers.binf.ku.dk/bloodspot). This database includes the original transcriptome analysis results of CBX4 and the CERS family in AML samples and normal samples. To validate the differential expression of ARG in AML versus normal samples, the GEPIA2 database (http://gepia2.cancer-pku.cn) was further utilized. Boxplots generated by the GEPIA2 database further confirmed the differential expression patterns predicted by Bloodspot analysis.

Cell culture

Human AML cell lines (THP-1 and KG-1) and the human hematopoietic stem cell line $CD34^+$ were all purchased from Precella Company (Virginia, USA). Cells were cultured in DMEM supplemented with 10% fetal bovine serum (FBS) and 1% penicillin/streptomycin (P/S). Growth factors were additionally supplemented for the $CD34^+$ cell line. THP-1 and KG-1 cell lines were passaged every two days, with medium replacement as needed based on cell density. $CD34^+$ cells were similarly passaged every two days, with culture duration limited to 7 days. Culture flasks were incubated in a constant-temperature incubator at 5% CO_2 and 37°C, and cells in the logarithmic growth phase were selected for subsequent experiments.

RNA extraction and sequencing

Total RNA was extracted from both cell lines and clinical samples using TRIzol reagent (Invitrogen). For RNA sequencing, RNA integrity was assessed using a Qubit fluorometer, and only samples with an RNA Integrity Number (RIN) ≥7.0 were used for library preparation. Paired-end sequencing was performed on the Illumina HiSeq™ 2000 platform.

Quantitative RT-PCR analysis

Following RNA extraction from both cellular and clinical samples, high-quality RNA was reverse-transcribed into cDNA using reverse transcriptase. Quantitative PCR amplification was performed with sequence-specific primers and SYBR Green master mix on a real-time PCR detection system. Relative gene expression was calculated using the $2^{-\Delta\Delta Ct}$ method after normalization to stably expressed reference genes.

Western blot analysis (WB)

Cell samples were washed with ice-cold phosphate-buffered saline (PBS), and total proteins were extracted using cell lysis buffer. The lysates were centrifuged at 12,000×g for 15 minutes at 4°C, and the supernatants were collected. Protein concentrations were determined using a BCA protein assay kit. Equal amounts of protein (40 μg) were separated by 15% SDS-PAGE and electrophoretically transferred to Millipore PVDF membranes. Immunoreactive proteins bound were visualized using an enhanced chemiluminescence (ECL) kit (Millipore). GAPDH served as the internal loading control, and all experiments were performed in triplicate.

Cell grouping

Gene knockdown models were established by transfecting siRNA targeting the gene of interest, while overexpression models were constructed using lentiviral infection. In the THP-1 cell line, the following groups were established: CBX4 knockdown group (si-CBX4), CBX4 overexpression group (oe-CBX4), CERS6 knockdown group (si-CERS6), HDAC5 knockdown group (si-HDAC5), SUMO inhibition group (ML-792), and RING1B knockdown group (si-RING1B. To further validate the functional role of CBX4, the si-CBX4 group was subdivided into several treatment subgroups: CERS6 overexpression group (si-CBX4+oe-CERS6), SUMO inhibition group (si-CBX4+ML-792), fumonisin

B1-induced ceramide synthesis inhibition group (si-CBX4+Inhibitor1), GW4869-induced ceramide synthesis inhibition group (si-CBX4+ Inhibitor2), and combined inhibition group (si-CBX4+Inhibitor1&2).

Cell proliferation assay

THP-1 cells was seeded into a 96-well plate at 100 μL per well and pre-cultured at 37°C in a 5% CO_2 atmosphere for 12-24 hours to allow cell adhesion. After attachment, the experimental groups were replaced with fresh medium containing specific drug concentrations, while the control groups were replaced with drug-free medium, followed by continued culture for the predetermined duration. Subsequently, 10 μL of CCK-8 solution was added to each well, ensuring gentle dispensing using pipette tip to avoid bubble formation. After uniform mixing, the plates were incubated at 37°C for 1-4 hours in the dark. Following incubation, the development of orange-yellow color in the wells was observed, and the absorbance was measured at 450 nm using a microplate reader.

Cell apoptosis assay

THP-1 cells were collected and centrifuged at 1000 rpm for 5 minutes, followed by wash with pre-cooled PBS for three times. After staining according to the manufacturer's protocol, residual antibodies were removed by washing twice with PBS. The cells were resuspended in 300-500 μL of PBS containing 1% BSA, filtered through a 300-mesh nylon membrane, and transferred into flow cytometry tubes for immediate analysis or storage at 4°C protected from light.

Cell cycle analysis

THP-1 cells were collected, centrifuged, and washed twice with pre-cooled PBS. The cell concentration was adjusted and then fixed with 70% ice-cold ethanol. After fixation, ethanol and cellular debris were thoroughly removed by centrifugation. Subsequently, the cells were then treated with RNase A and stained with propidium iodide (PI). Red fluorescence was detected using a BD FACSAria III flow cytometer (BD Biosciences), and cell cycle distribution was analyzed based on DNA content.

Lipidomic analysis

THP-1 cell samples were mixed with an internal standard extraction solution, vortexed, and centrifuged. The supernatant was collected for liquid chromatography-tandem mass spectrometry (LC-MS/MS) analysis. Chromatographic separation was performed on a Thermo Accucore™ C30 column using a gradient elution at a flow rate of 0.35 mL/min and an injection volume of 2 μL. Mass spectrometry was conducted with an electrospray ion source, with the mass spectrometry voltage set to 5500 V in positive ion mode and -4500 V in negative ion mode. The curtain gas was set to 45 psi (Gas 1) and 55 psi (Gas 2), and the collision-induced ionization parameter was set to a medium level. The CDS 3.1 data processing software was used to integrate the detected chromatographic peaks for quantification. The quantitative results were normalized, and both qualitative and quantitative lipidomic analyses were performed.

Proteomic analysis

Proteomic analysis was performed using a mass spectrometry-based quantitative approach. Total proteins were first extracted from cells via ultrafiltration concentration and acetone precipitation, followed by reduction, alkylation, and tryptic digestion to generate peptides. Mass spectrometric analysis was carried out on a timsTOF Pro instrument equipped with a CaptiveSpray nano-electrospray ion source. Data-independent acquisition (DIA) was performed using the diaPASEF method to simultaneously obtain high-accuracy mass spectral information for both precursor and fragment ions. Finally, the DIA-NN software was used to match the raw mass spectrometry data against the UniProt human protein sequence database.

Cleavage under targets and tagmentation (CUT&Tag)

Intact cells were immobilized using concanavalin A-coated magnetic beads. After permeabilization, target protein-specific primary antibodies and Protein A-Tn5 transposase complexes were sequentially added to precisely localize the transposase to antibody-bound chromatin regions. Magnesium ions were then introduced to activate the transposase, enabling simultaneous DNA cleavage and sequencing adapter ligation at target sites. The reaction was terminated, and tagmented DNA fragments were released by Proteinase K digestion. Following purification, indexed primers were used for PCR

Table 1. Baseline characteristics of the clinical samples

Characteristics	AML (n=50)	Control (n=50)	$t/\chi^2/Z$	*P*
Sex, n (%)			0.367	0.545
Male	30 (60.00)	27 (54.00)		
Female	20 (40.00)	23 (46.00)		
Age, years, ($\bar{x}$±s)	53.14±11.94	50.17±11.06	1.290	0.200
FAB classification, n (%)			/	/
M3	8 (16.00)	/		
M5	42 (84.00)	/		
Specimen type, n (%)			21.951	0.000
Peripheral blood	32 (64.00)	50 (100.00)		
Bone marrow	18 (36.00)	0 (0.00)		
WBC, $\times10^9$/L, [M (P_{25}, P_{75})]	13.52 (9.41, 17.86)	16.82 (9.32, 20.41)	2.074	0.038
HGB, g/L, [M (P_{25}, P_{75})]	83.15 (43.17, 126.59)	91.06 (44.79, 131.86)	0.812	0.417
PLT, $\times10^9$/L, [M (P_{25}, P_{75})]	37.61 (5.26, 197.62)	30.41 (5.18, 189.37)	0.357	0.721
LDH, IU/L, [M (P_{25}, P_{75})]	612.15 (189.59, 6142.07)	684.66 (183.01, 6187.72)	0.109	0.913

WBC: White blood cell count. HGB: Hemoglobin. PLT: Platelet count. LDH: Lactate dehydrogenase.

amplification to construct sequencing libraries suitable for high-throughput analysis.

Co-Immunoprecipitation (Co-IP)

Cells were lysed under non-denaturing conditions to preserve native protein-protein interactions. After pre-clearing, the lysate was incubated overnight at 4°C with a specific antibody against the "bait" protein. Protein A/G magnetic beads were then added to capture antibody-antigen complexes, followed by multiple washes to remove non-specific binding. Finally, the complexes were eluted by boiling and analyzed by Western Blotting to detect the "prey" protein. An isotype IgG was used as a negative control, and input lysate served as a positive reference to verify interaction specificity.

Dual-luciferase reporter experiment

THP-1 cells were first transfected with a luciferase reporter gene, followed by co-transfection with siRNA. Cells were harvested 24 hours post-transfection and analyzed using the Dual-Luciferase Reporter Assay System (Beyotime Biotechnology, Cat. No. RG027).

Statistical analysis

All bioinformatics and statistical analyses were performed in the R environment. The *limma* package was employed for normalization and differential expression analysis of raw sequencing data, with thresholds set at |log2FC|>1 and adjusted *P*<0.05. KEGG pathway enrichment analysis of differentially expressed genes (DEGs) was conducted using the *clusterProfiler* package (*enrichKEGG* function), and visualization was performed using *ggplot2*. All statistical analyses were conducted using SPSS 26.0, and graphs were generated using GraphPad Prism (version 9.0). The Shapiro-Wilk test was applied to assess normality. Normally distributed continuous variables were expressed as mean ± standard deviation ($\bar{x}$±s) and compared using the independent samples t-test. Non-normally distributed data were presented as median (P_{25}, P_{75}) and analyzed using the Mann-Whitney U test. Categorical variables were described as n (%) and compared using the χ^2 test. *P*<0.05 was considered statistically significant.

Results

Baseline characteristics of clinical samples

No significant differences were observed between the AML and control groups in baseline characteristics including sex, age, hemoglobin (HGB), platelet count (PLT), and lactate dehydrogenase (LDH) (all *P*>0.05). However, significant differences were found in white blood cell count (WBC) and sample type (*P*<0.05) (**Table 1**).

Expression profiles of CERS and CBX4 in AML databases

Analysis of the BloodSpot database revealed that the expression levels of CERS1-CERS5

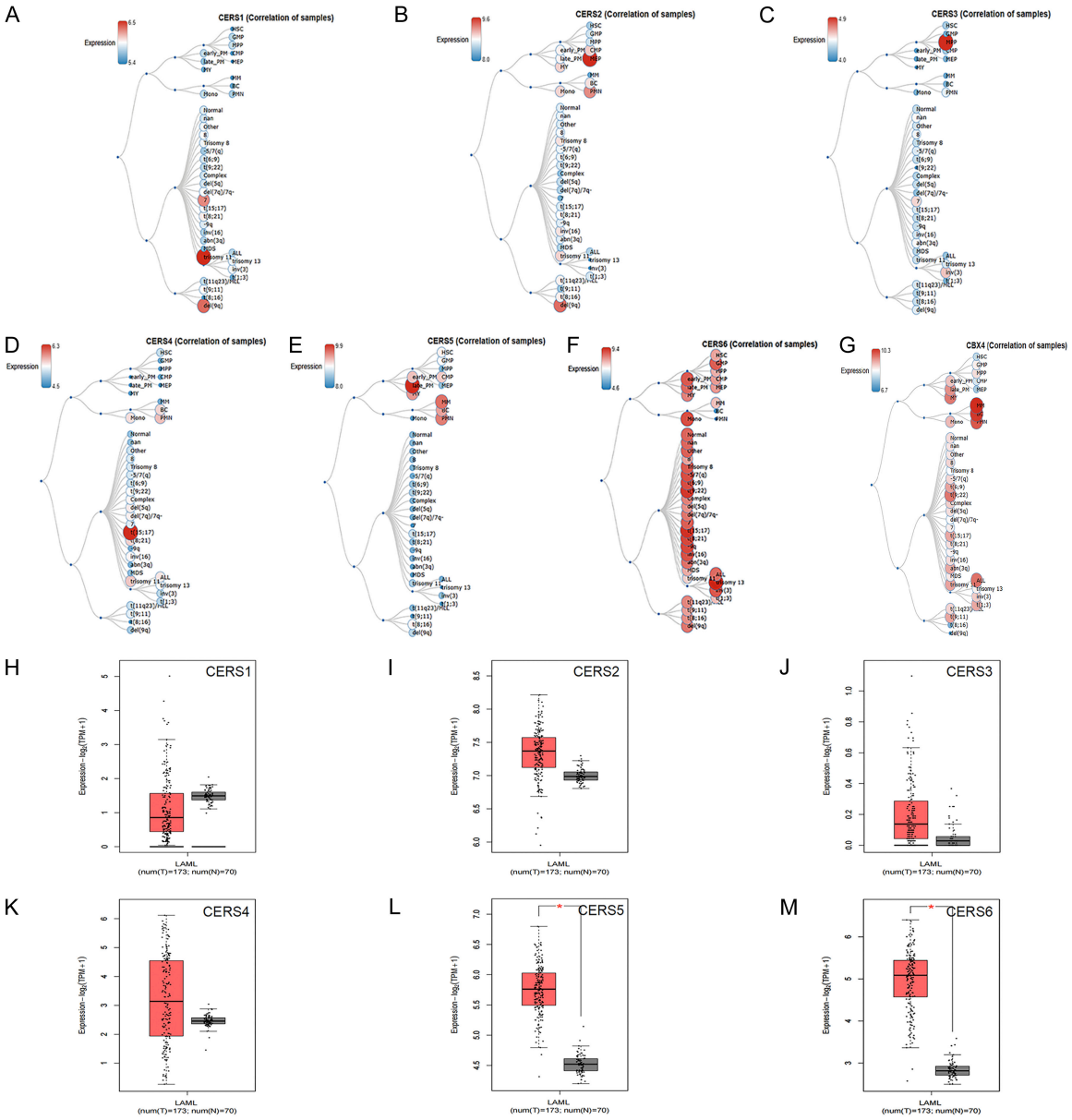

Figure 1. The expression profile of CBX4 and CERS in AML from database. Note: (A-F) CERS1-CERS6 expression profiles across AML karyotypes analyzed via Bloodspot database. (G) CBX4 expression profiles across AML karyotypes analyzed via Bloodspot database. (H-M) Analysis of CERS1-CERS6 expression in AML vs. Normal Controls via GEPIA2 database. *P<0.05.

remained largely unchanged across different AML karyotypes (**Figure 1A-E**), whereas the expression level of CERS6 was significantly elevated in various AML karyotypes (**Figure 1F**). The expression level of CBX4 also elevated across AML karyotypes (**Figure 1G**). Further validation using the GEPIA2 database showed that CERS1-4 expression did not differ significantly between normal and AML samples (P>0.05) (**Figure 1H-K**), while CERS5 and CERS6 expression levels were significantly elevated in AML samples (P<0.05) (**Figure 1L**, **1M**).

Expression profiles across cell lines and clinical validation

Transcriptome sequencing results of THP-1 and CD34$^+$ cell lines showed that the CBX family members were expressed in both cell lines, and CBX4 showing markedly higher expression in THP-1 cells than CD34$^+$ cells (**Figure 2A**). qPCR and Western blot analyses confirmed that both mRNA and protein expression of CBX4 were upregulated in THP-1 and KG-1 cell lines (**Figure 2B**, **2C**). Clinical sample validation further sup-

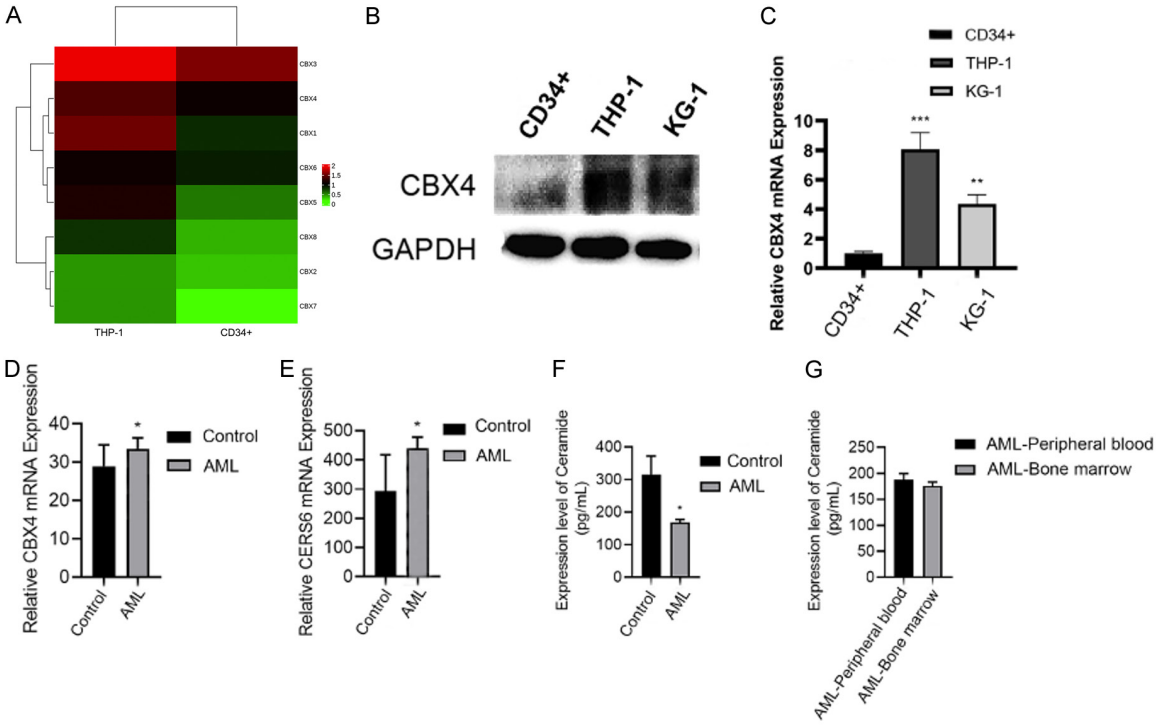

Figure 2. Expression profiles across cell lines and clinical validation. Note: (A) Sequencing results of THP-1 and CD34$^+$ cell lines. (B) Protein expression of CBX4 in three cell lines. (C) mRNA expression of CBX4 in three cell lines. (D) mRNA expression of CBX4 in different clinical samples. (E) mRNA expression of CERS6 in different clinical samples. (F) Ceramide expression in different clinical samples. (G) Ceramide expression in different sample types from AML patients. $^*P<0.05$, $^{**}P<0.01$, $^{***}P<0.001$.

ported these findings: qPCR showed that the expression levels of CBX4 and CERS6 in the AML group were significantly higher than those in the control group ($P<0.05$) (**Figure 2D**, **2E**). LC-MS/MS analysis revealed that ceramide levels were significantly reduced in the AML group compared to the control group ($P<0.05$), but no significant difference was observed between bone marrow and peripheral blood samples within the AML group ($P>0.05$) (**Figure 2F**, **2G**).

Validation of the cell model

In the THP-1 cell line, both protein and mRNA expression of CBX4 in the si-CBX4 group were significantly decreased compared to the NC group ($P<0.05$) (**Figure 3A**, **3B**). In contrast, these levels in the oe-CBX4 group were significantly increased compared to the NC group ($P<0.05$) (**Figure 3C**, **3D**). After 48, 60, and 72 hours of culture, THP-1 cell proliferation was significantly enhanced in the si-CBX4 group compared to the NC group ($P<0.05$) (**Figure 3E**). No significant change in THP-1 cell proliferation was observed in the oe-CBX4 group compared to the NC group ($P>0.05$) (**Figure 3F**). Cell apoptosis in the si-CBX4 group showed no significant difference compared to the NC group ($P>0.05$) (**Figure 3G**, **3H**). The expression of cell cycle-related proteins CCND1, CCND2, CCND3, and CDK4 in the si-CBX4 group was significantly elevated compared to the NC group ($P<0.05$) (**Figure 3I**). Furthermore, THP-1 cells in the si-CBX4 group exhibited shortened G1 phase and prolonged S phase (**Figure 3J**, **3K**). However, no significant differences in cell cycle-related protein expression were detected in the oe-CBX4 group compared to the NC group ($P>0.05$) (**Figure 3L**).

Lipid metabolism

Quantitative lipidomic analysis identified a total of 847 lip metabolites in THP-1 cells from the si-CBX4 group (**Figure 4A**). These were primarily categorized into six major classes: sterol lipids (ST), SP, prenol lipids (PR), glycerophospholipids (GP), glycerolipids (GL), and fatty acids (FA), with GP, GL, and SP being the most abundant (**Figure 4B**). A total of 170 differentially expressed lipid molecules were identified, of which 63 were up-regulated and 107 were

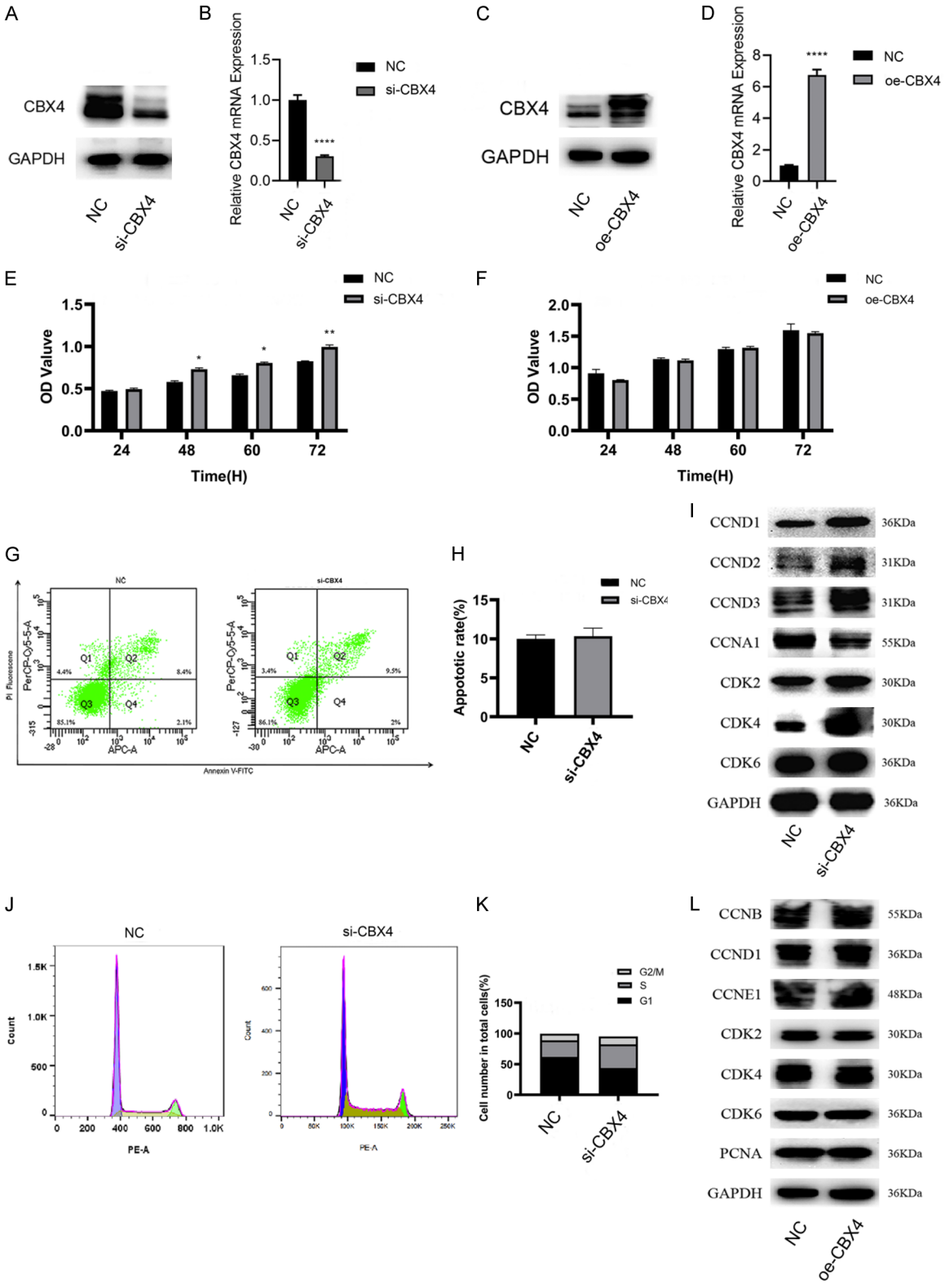

Figure 3. Validation of the cell model. Note: (A) Protein expression in the CBX4 knockdown model. (B) mRNA expression in the CBX4 knockdown model. (C) Protein expression in the CBX4 overexpression model. (D) mRNA expression in the CBX4 overexpression model. (E) CCK-8 results of the CBX4 knockdown model. (F) CCK-8 results of the CBX4 overexpression model. (G, H) Cell apoptosis assay in the CBX4 knockdown model. (I) Expression of cycle-related proteins in the CBX4 knockdown model. (J, K) Cell cycle detection in the CBX4 knockdown model. (L) Expression of cell cycle-related proteins in the CBX4 overexpression model. $^{*}P<0.05$, $^{**}P<0.01$, $^{****}P<0.0001$.

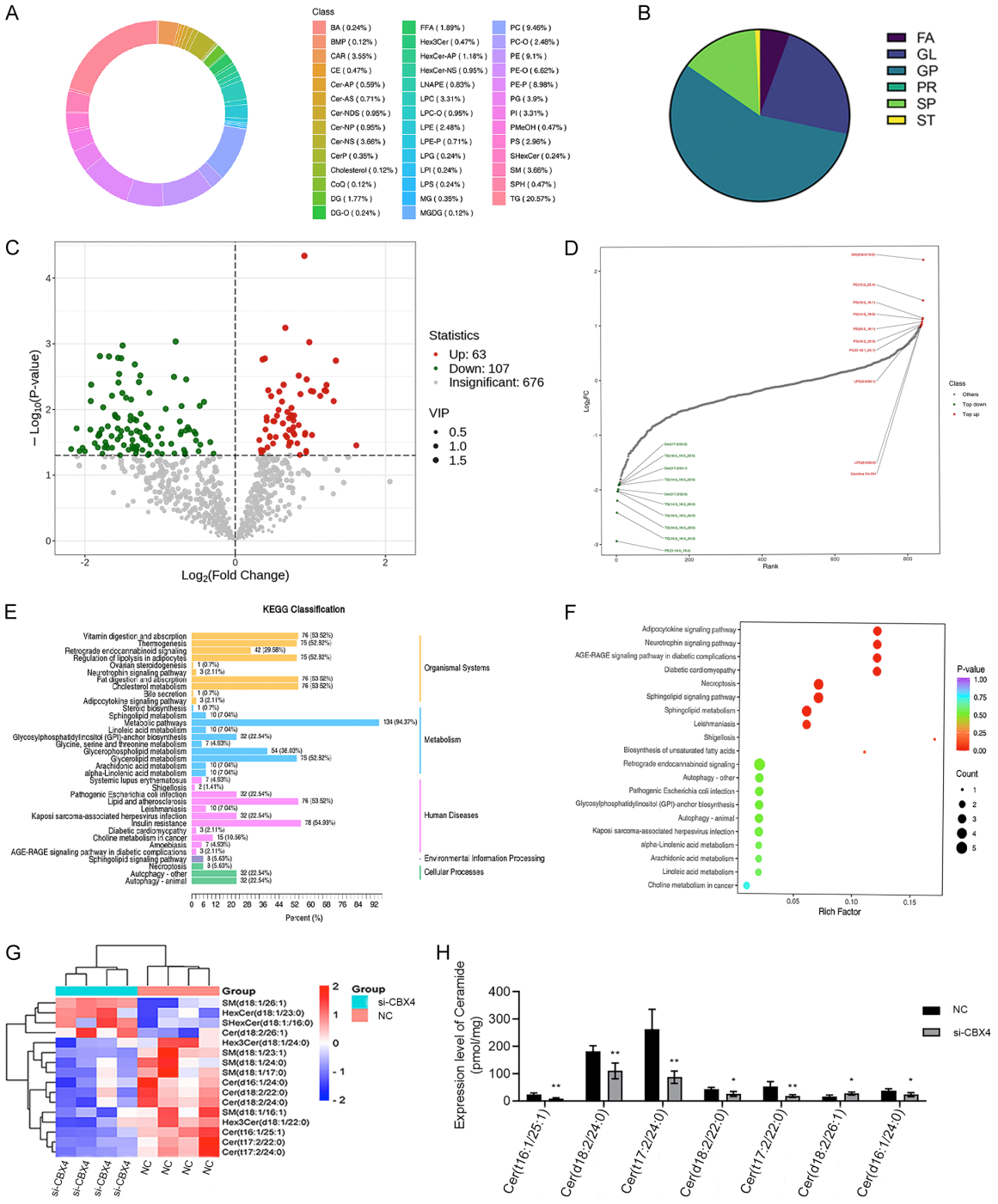

Figure 4. Lipid metabolism. Note: (A) Diagram of lipid subclass composition. (B) Pie chart of lipid classification. (C) Volcano plot of quantitative lipids. (D) Top 10 up-regulated and down-regulated lipids. (E) KEGG enrichment of differentially expressed lipids. (F) KEGG classification chart of differentially expressed lipids. (G) Heatmap of differentially expressed lipids. (H) Differential expression of ceramide molecules among differential lipids. $^{*}P<0.05$, $^{**}P<0.01$.

down-regulated. The top 10 up-regulated and down-regulated lipid molecules were analyzed (**Figure 4C**, **4D**). KEGG enrichment and classification analysis of the differentially expressed lipid molecules indicated that SP metabolism and adipocytokine signaling pathway were the most significantly affected (**Figure 4E**, **4F**). The expression of lipid molecules in THP-1 cells of the si-CBX4 group showed overall differences compared to the NC group. Except for

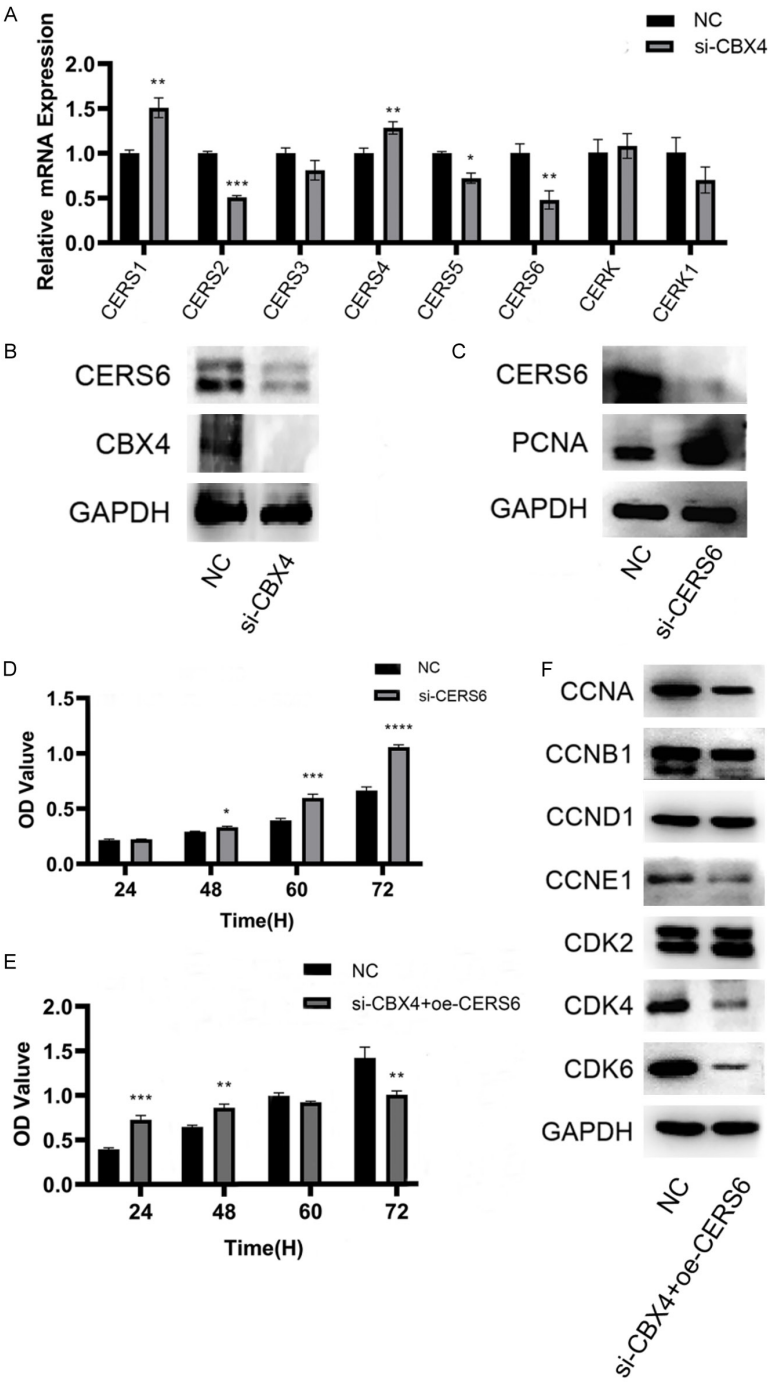

Figure 5. CBX4 positively regulates CERS6. Note: (A) mRNA expression of the CERS family in the si-CBX4 group. (B) CERS6 protein expression in the si-CBX4 group. (C) Expression of cell proliferation proteins in the si-CERS6 group. (D) CCK-8 results of the si-CERS6 group. (E) CCK-8 results of the si-CBX4+oe-CERS6 group. (F) Expression of cell cycle-related proteins in the si-CBX4+oe-CERS6 group. **P*<0.05, ***P*<0.01, ****P*<0.001, *****P*<0.0001.

Cer(d18:2/26:1), the expression of ceramide molecules in the si-CBX4 group was significantly lower than that in the NC group (*P*<0.05) (**Figure 4G**, **4H**).

CBX4 positively regulates CERS6

Both CERS6 mRNA and protein expression levels in the si-CBX4 group were significantly decreased compared to the NC group (*P*<0.05) (**Figure 5A**, **5B**). The expression of PCNA, a marker of cell proliferation activity, was significantly upregulated in the si-CERS6 group compared to the NC group (*P*<0.05) (**Figure 5C**). Cell proliferation in the si-CERS6 group increased significantly over time and was markedly higher than that in the NC group (*P*<0.05) (**Figure 5D**). In contrast, cell proliferation in the si-CBX4+oe-CERS6 group was significantly decreased compared to the NC group after 60 hours (*P*<0.05) (**Figure 5E**). Furthermore, the expression of cell cycle-related proteins in the si-CBX4+oe-CERS6 group was reduced relative to the NC group (**Figure 5F**).

Proteomic analysis

By constructing mutants of CBX4, the aim was to investigate the protein modification mechanisms between CBX4 and CERS6. The protein domain results are shown in **Figure 6A**. In the ΔCDM mutant, H3K27me3 protein expression was decreased, while SUMO1 and CERS6 protein expression were significantly increased (*P*<0.05) (**Figure 6B**). The gene expression levels in the si-CBX4 group were generally higher than those in the NC group (**Figure 6C**). KEGG pathway enrichment analysis indicated primary regulation of nicotinate and nicotinamide metabolism and cholesterol metabolism (**Figure 6D**). Compared to the NC group, the expression of lipid-related DEGs in the si-CBX4

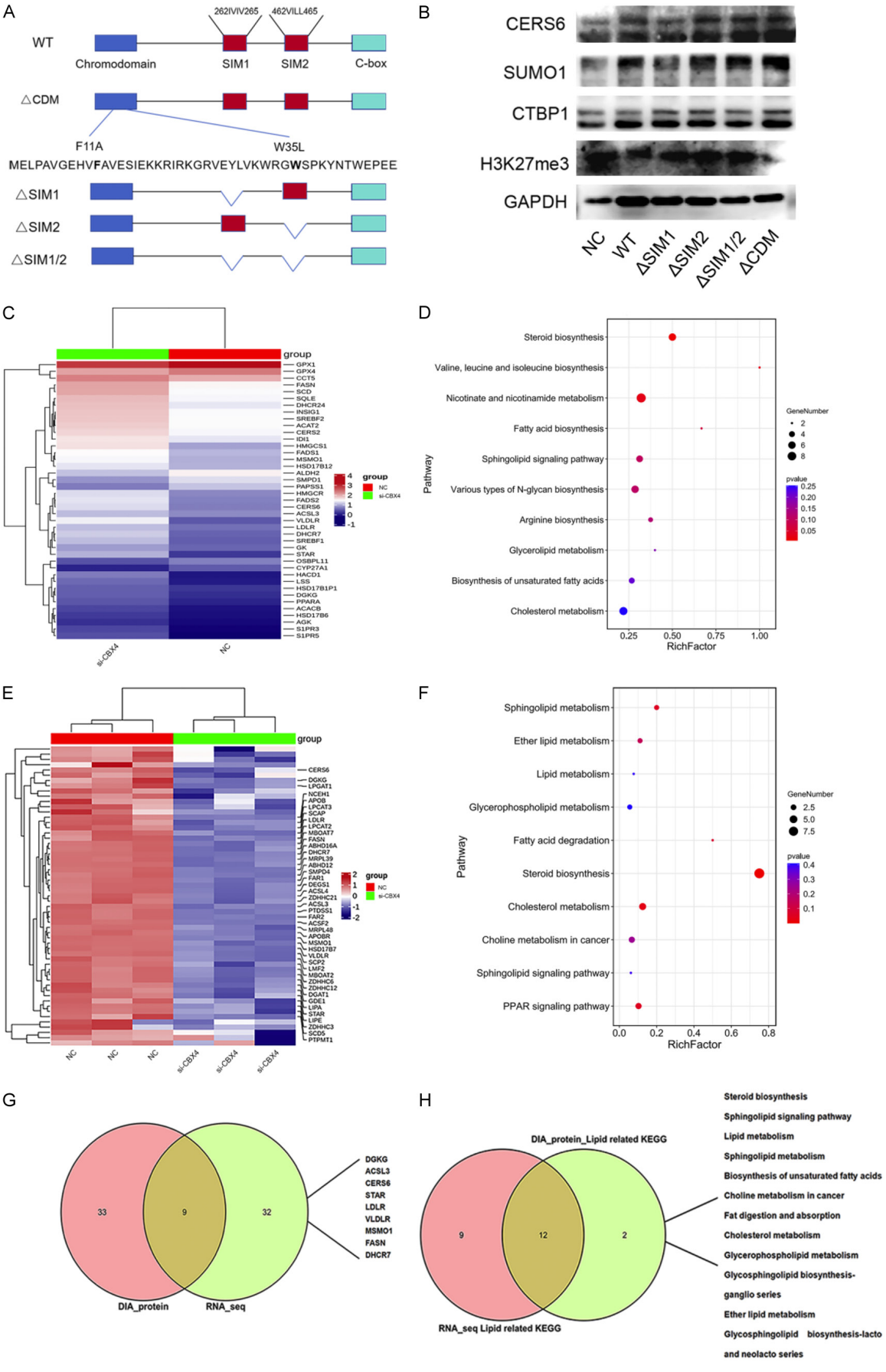
A
WT
262IVIV265
462VILL465
Chromodomain
SIM1
SIM2
C-box
△CDM
F11A
W35L
MELPAVGEHVFAVESIEKKRIRKGRVEYLVKWRGWSPKYNTWEPEE
△SIM1
△SIM2
△SIM1/2
B
CERS6
SUMO1
CTBP1
H3K27me3
GAPDH
NC
WT
ΔSIM1
ΔSIM2
ΔSIM1/2
ΔCDM
C
group
NC
si-CBX4
D
Steroid biosynthesis
Valine, leucine and isoleucine biosynthesis
Nicotinate and nicotinamide metabolism
Fatty acid biosynthesis
Sphingolipid signaling pathway
Various types of N-glycan biosynthesis
Arginine biosynthesis
Glycerolipid metabolism
Biosynthesis of unsaturated fatty acids
Cholesterol metabolism
Pathway
RichFactor
GeneNumber
pvalue
E
group
F
Sphingolipid metabolism
Ether lipid metabolism
Lipid metabolism
Glycerophospholipid metabolism
Fatty acid degradation
Steroid biosynthesis
Cholesterol metabolism
Choline metabolism in cancer
Sphingolipid signaling pathway
PPAR signaling pathway
Pathway
RichFactor
GeneNumber
pvalue
G
33
9
32
DIA_protein
RNA_seq
DGKG
ACSL3
CERS6
STAR
LDLR
VLDLR
MSMO1
FASN
DHCR7
H
DIA_protein_Lipid related KEGG
9
12
2
RNA_seq Lipid related KEGG
Steroid biosynthesis
Sphingolipid signaling pathway
Lipid metabolism
Sphingolipid metabolism
Biosynthesis of unsaturated fatty acids
Choline metabolism in cancer
Fat digestion and absorption
Cholesterol metabolism
Glycerophospholipid metabolism
Glycosphingolipid biosynthesis-ganglio series
Ether lipid metabolism
Glycosphingolipid biosynthesis-lacto and neolacto series

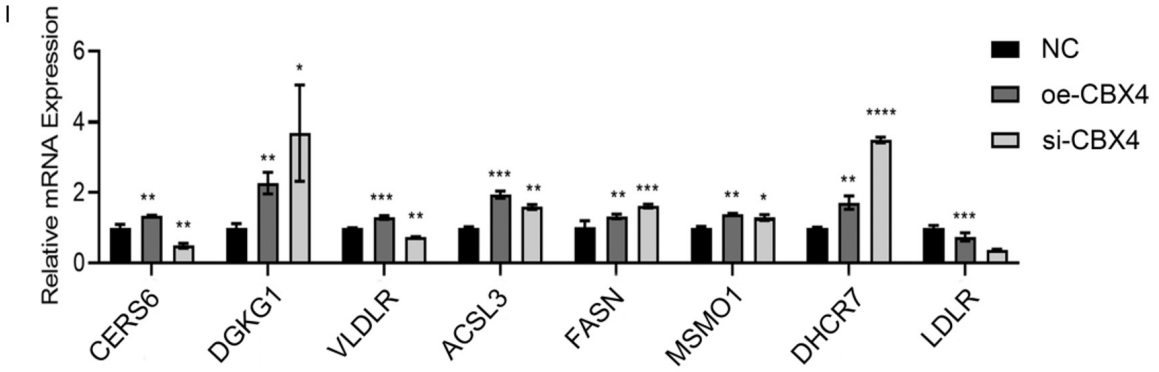

Figure 6. Proteomic analysis. Note: (A) CBX4 protein domains. (B) CBX4 protein modification. (C) Proteomic analysis of differential genes regulated by CBX4. (D) KEGG pathway enrichment analysis of CBX4-regulated signaling cascades. (E) Proteomic profiling of CBX4-controlled lipid-metabolism genes. (F) KEGG lipid-metabolism pathway enrichment analysis. (G) Lipid-metabolism-related genes. (H) Lipid-metabolism-associated pathways. (I) qPCR quantification of mRNA expression of lipid-metabolism gene. $^{*}P<0.05$, $^{**}P<0.01$, $^{***}P<0.001$, $^{****}P<0.0001$.

group was significantly decreased (**Figure 6E**). KEGG pathway enrichment analysis revealed primary regulation of steroid biosynthesis (**Figure 6F**). This involved 9 DEGs and 12 KEGG pathways related to lipid metabolism (**Figure 6G**, **6H**). Compared to the NC group, both the oe-CBX4 and si-CBX4 groups showed significant differences in the expression of lipid metabolism-related genes ($P<0.05$) (**Figure 6I**).

CBX4 targets CERS6 and its regulatory role

CUT&Tag analysis precisely identified the chromatin binding sites between CBX4 and CERS6 (**Figure 7A**), while Co-IP further validated their targeting relationship (**Figure 7B**). With increasing concentration of the SUMOylation inhibitor ML-792, SUMO2/3 protein expression correspondingly decreased, while SUMO1 protein expression was completely abolished (**Figure 7C**). In the si-CBX4+ML-792 group, elevated inhibitor concentrations led to partial restoration of SUMO1 protein expression, accompanied by a gradual increase in SUMO2/3 expression (**Figure 7D**). In the si-RING1B group, protein expression levels of CBX4, CERS6, and RING1B showed no significant changes compared to the NC group (**Figure 7E**). The protein expression of RING1B in the si-CBX4+si-RING1B group was significantly decreased compared to the NC group (**Figure 7F**).

CBX4 interacts with HDAC5 to regulate CERS6

CUT&Tag analysis identified the binding sites between CBX4 and HDAC5 (**Figure 8A**), while Co-IP further validated the targeting of the HDAC family by CBX4 (**Figure 8B**). The HDAC5 mRNA expression was significantly increased in the si-CBX4 group ($P<0.05$) and significantly decreased in the oe-CBX4 group ($P<0.05$) (**Figure 8C**). HDAC5 protein expression was significantly elevated in the si-CBX4 group (**Figure 8D**). Co-IP further confirmed the mutual targeting relationship between HDAC5 and CERS6 (**Figure 8E**). CERS6 was found to interact with HDAC family proteins (**Figure 8F**). CERS6 protein expression was significantly upregulated in the si-HDAC5 group ($P<0.05$) (**Figure 8G**). The reciprocal targeting between HDAC5 and CBX4 was further verified by Co-IP (**Figure 8H**). In the si-HDAC5 group, cell proliferation increased gradually over time. However, starting from 48 hours, the cell proliferation in the si-HDAC5 group was significantly lower than that in the control group ($P<0.05$) (**Figure 8I**).

Dual-luciferase assay was performed to verify the transcriptional regulatory role of HDAC5

The regulatory relationship between HDAC5 and CERS6 was verified by dual-luciferase assay. The promoter plasmid was constructed, and compared to the empty promoter group, the luciferase activity was significantly enhanced ($P<0.05$) in untreated THP-1 cells, suggesting increased HDAC5 promoter activity (**Figure 9A**). In contrast, the luciferase activity was markedly reduced in si-CBX4 THP-1 cells, with a significant decrease in HDAC5 promoter activity (P<0.05) (**Figure 9B**).

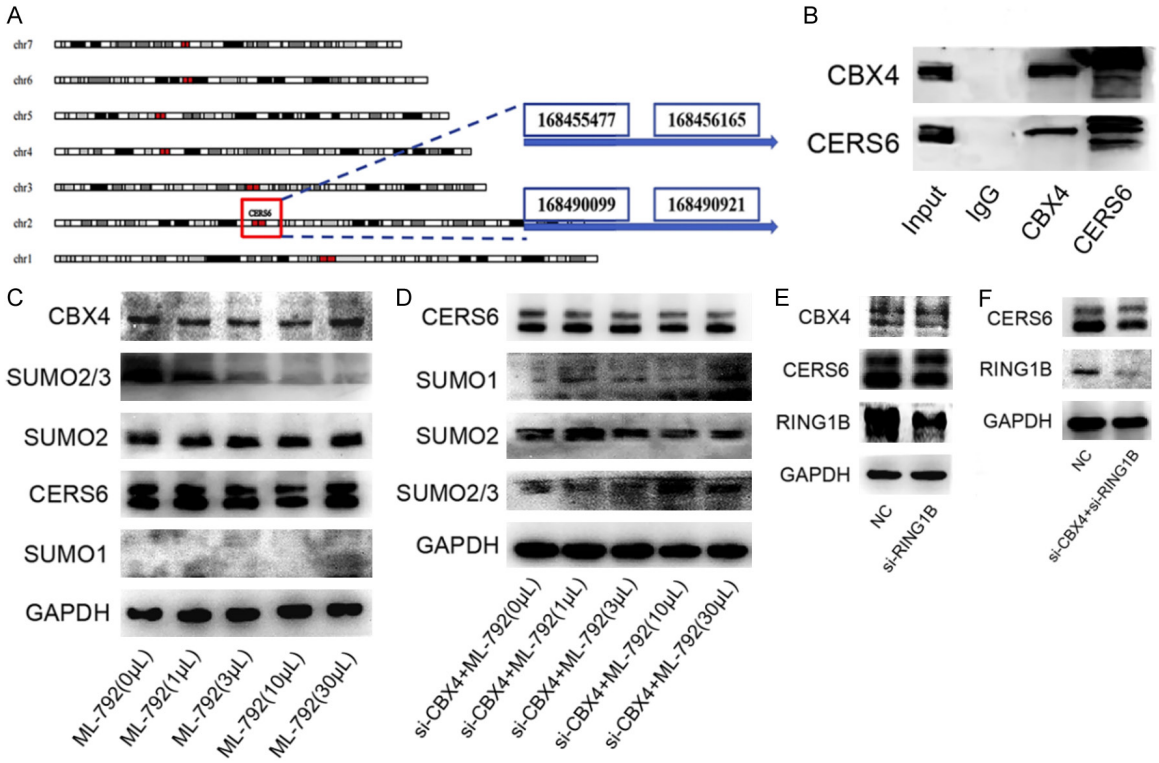

Figure 7. CBX4 targets CERS6 and its regulatory role. Note: (A) CUT&Tag to identify the binding sites between CBX4 and CERS6. (B) Co-IP analysis of the interaction between CBX4 and CERS6. (C) WB results of SUMOylation inhibition at different concentrations. (D) WB results of si-CBX4 combined with SUMOylation inhibition at different concentrations. (E) Detection of related protein expression after inhibition of SUMOylation modification targets. (F) Detection of related protein expression after si-CBX4 combined with inhibition of SUMOylation modification targets.

The role of CBX4 in ceramide regulation

KEGG pathway enrichment analysis of RNA sequencing and proteomics data revealed that CBX4 is involved in regulating multiple lipid metabolism and acetylation signaling pathways (**Figure 10A**, **10B**). Compared to the NC group, the protein expression of PP2A, CBX4, and CERS6 was downregulated in the si-CBX4, si-CBX4+Inhibitor1, si-CBX4+Inhibitor2, and si-CBX4+Inhibitor1&2 groups. Notably, the downregulation of CBX4 protein expression was more pronounced in the si-CBX4+Inhibitor2 and si-CBX4+Inhibitor1&2 groups. Conversely, PCNA protein expression was upregulated in all four groups, with a more marked upregulation observed in the si-CBX4+Inhibitor2 and si-CBX4+Inhibitor1&2 groups (**Figure 10C**, **10D**). Analysis of key proteins regulating cell growth and survival signaling pathways in SP metabolism showed that si-CBX4 induced the activation of p-AKT/p-PI3K and p-MEK1/2/p-Raf1. A synergistic enhancement in the activation of p-AKT/p-PI3K, p-MEK1/2, and p-Raf1 was observed when CBX4 knockdown was combined with inhibitor treatment (**Figure 10E**, **10F**).

Discussion

Targeted drug therapy remains the primary treatment approach for AML, however, patient prognosis remains unsatisfactory [21]. The rapid proliferation of AML cells results in significant alterations in their metabolic characteristics, and aberrant metabolic patterns not only support leukemic cell survival but also contribute to drug resistance, thereby influencing treatment outcomes [22]. In recent years, researchers have shifted their focus toward targeted therapies related to lipid metabolism.

Both bioinformatics analyses and clinical samples have revealed that compared to normal samples, AML samples exhibit a significant downregulation in the expression of both CBX4 and CERS6, accompanied by a marked reduction in free ceramide levels [22, 23]. This con-

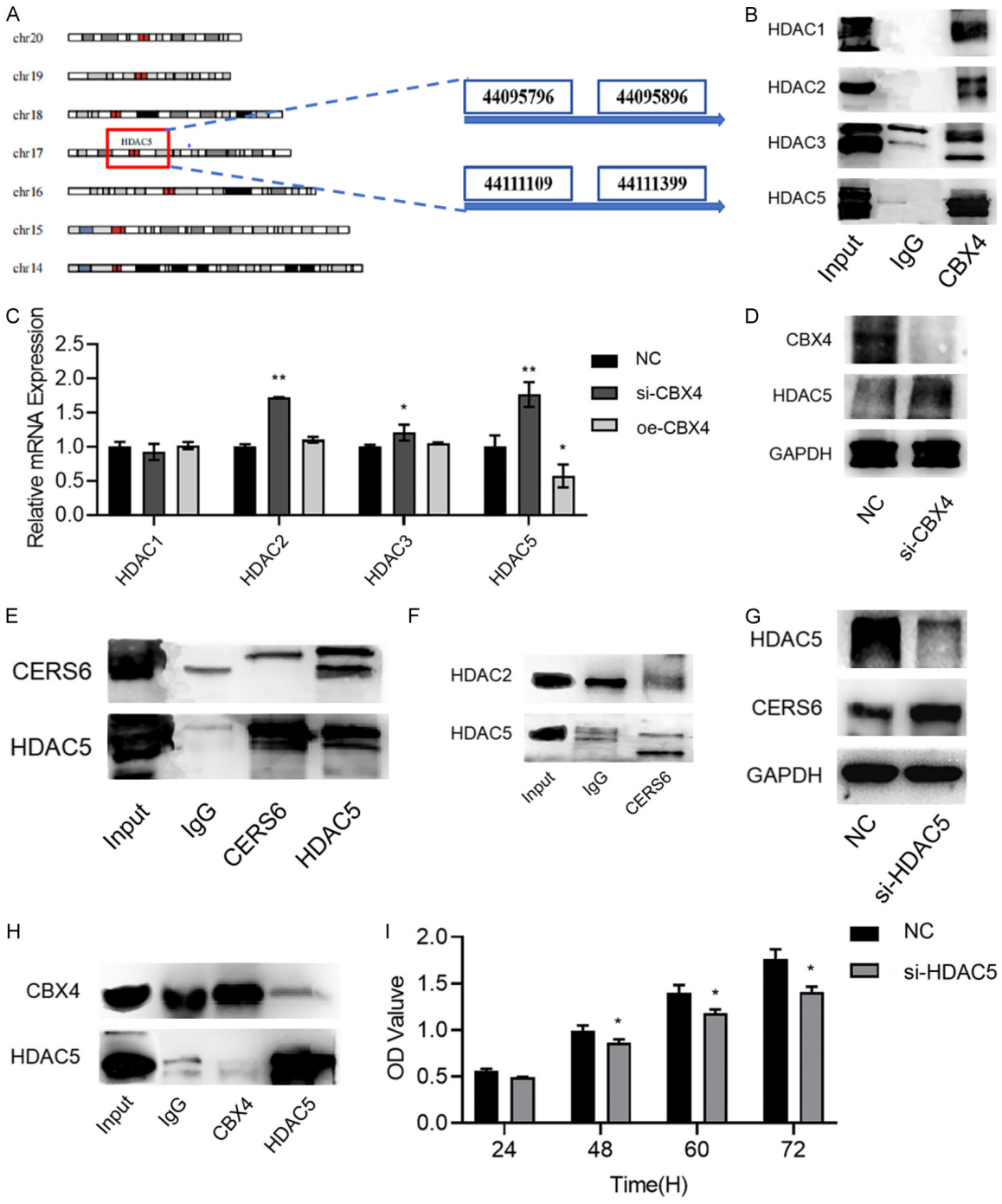

Figure 8. CBX4 interacts with HDAC5 to regulate CERS6. Note: (A) CUT&Tag to identify the binding sites of CBX4 and HDAC5. (B) Co-IP analysis of the interaction between CBX4 and HDAC family. (C) qPCR was performed to detect the mRNA expression of the HDAC family. (D) si-CBX4 was used to regulate HDAC5 protein expression. (E) Co-IP was employed to analyze the targeting of CERS6 by HDAC5. (F) Co-IP was used to examine the targeting of the HDAC family by CERS6. (G) si-HDAC5 was applied to regulate CERS6 protein expression. (H) Co-IP was conducted to validate the targeting relationship between CBX4 and HDAC5. (I) CCK-8 assay was performed to assess the effects of si-HDAC5. $^{*}P<0.05$, $^{**}P<0.01$.

sistent expression pattern suggests that CBX4 and CERS6 may jointly participate in the regulatory network of ceramide metabolic dysregulation in AML. In tumor metabolic reprogramming,

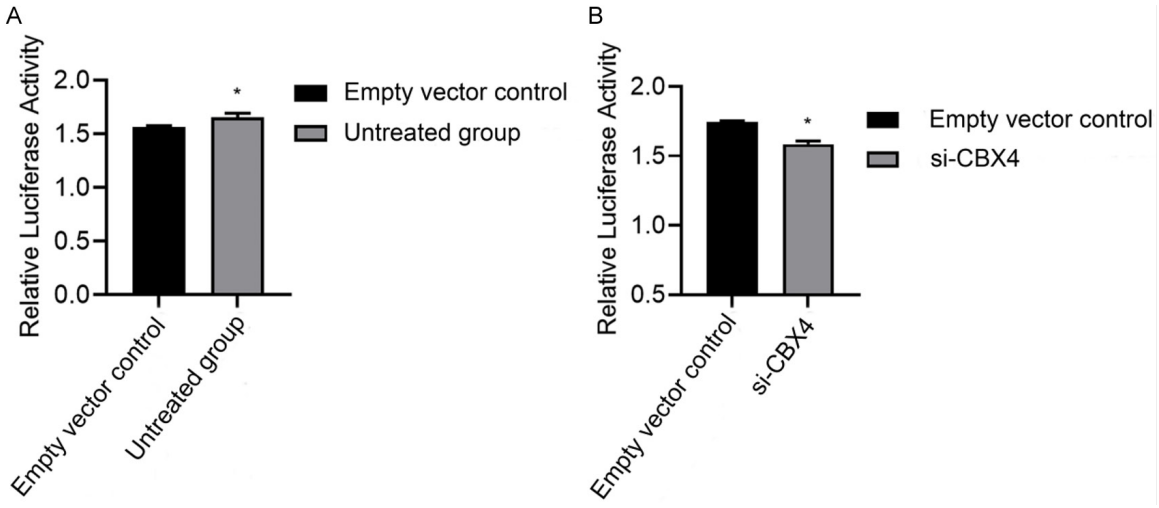

Figure 9. Dual-luciferase assay was performed to verify the transcriptional regulatory role of HDAC5. Note: (A) The transcriptional regulatory effect of HDAC5 on CERS6 was verified by dual-luciferase assay, (B) The transcriptional regulatory effect of CBX4 on HDAC5 was also verified by dual-luciferase assay. $^{*}P<0.05$.

HDAC family members often serve as key executors of epigenetic regulation, involved in the regulatory cascade linking CBX4 downregulation and reduced CERS6 expression [24]. Studies have shown that CBX4 can recruit HDAC5 to specific gene promoter regions, thereby influencing downstream gene transcription [14, 25]. As HDAC5 also plays an important role in SP metabolism, it is likely to function as a bridging molecule between CBX4 and CERS6, coordinating the signaling between epigenetic alterations and metabolic remodeling [26]. Subsequent cellular validation further verified the precise role of HDAC5 within this regulatory axis, providing a new theoretical foundation for therapeutic strategies targeting SP metabolism in AML.

Based on our apoptosis study, no significant increase in apoptosis was observed in the si-CBX4 group, a phenomenon that may be related to the inherent apoptosis resistance characteristics of AML cells. Research indicates that leukemia stem cells often establish robust anti-apoptotic barriers through mechanisms such as upregulating anti-apoptotic BCL-2 proteins, and CBX4 knockdown alone may be insufficient to overcome this barrier [27]. Cell proliferation in the si-CBX4 group was significantly enhanced after 48, 60, and 72 hours of culture. As an epigenetic regulator, CBX4 knockdown may directly upregulate cyclin expression by relieving transcriptional repression of cell cycle-related genes. Furthermore, our preliminary research suggests that disruption of the CBX4-HDAC5-CERS6 axis may lead to ceramide metabolism disorders, thereby affecting downstream proliferative signaling pathways [19]. As an important lipid second messenger, decreased ceramide levels may relieve the inhibition of pro-survival pathways, thus promoting cell proliferation [28]. The cell cycle reprogramming induced by CBX4 knockdown may reflect unique metabolic adaptation strategies of AML cells. Rapidly proliferating leukemia cells need to reconfigure their metabolic networks to meet biosynthetic demands, and the lipid metabolism pathways regulated by CBX4 may play a key role in this process [29]. In summary, CBX4 demonstrates unique functional complexity in AML - while its knockdown does not directly affect apoptosis, but significantly promotes cell proliferation by regulating cell cycle progression and metabolic reprogramming. These findings provide a theoretical basis for developing novel therapeutic strategies targeting this pathway.

Lipidomic analysis revealed that CBX4 knockdown led to significant alterations in the overall lipid profile of THP-1 cells, with the SP metabolism pathway being the most significantly disturbed. Specifically, the expression levels of multiple long-chain ceramide molecules were significantly downregulated, confirming that CBX4 is an important regulatory factor in main-

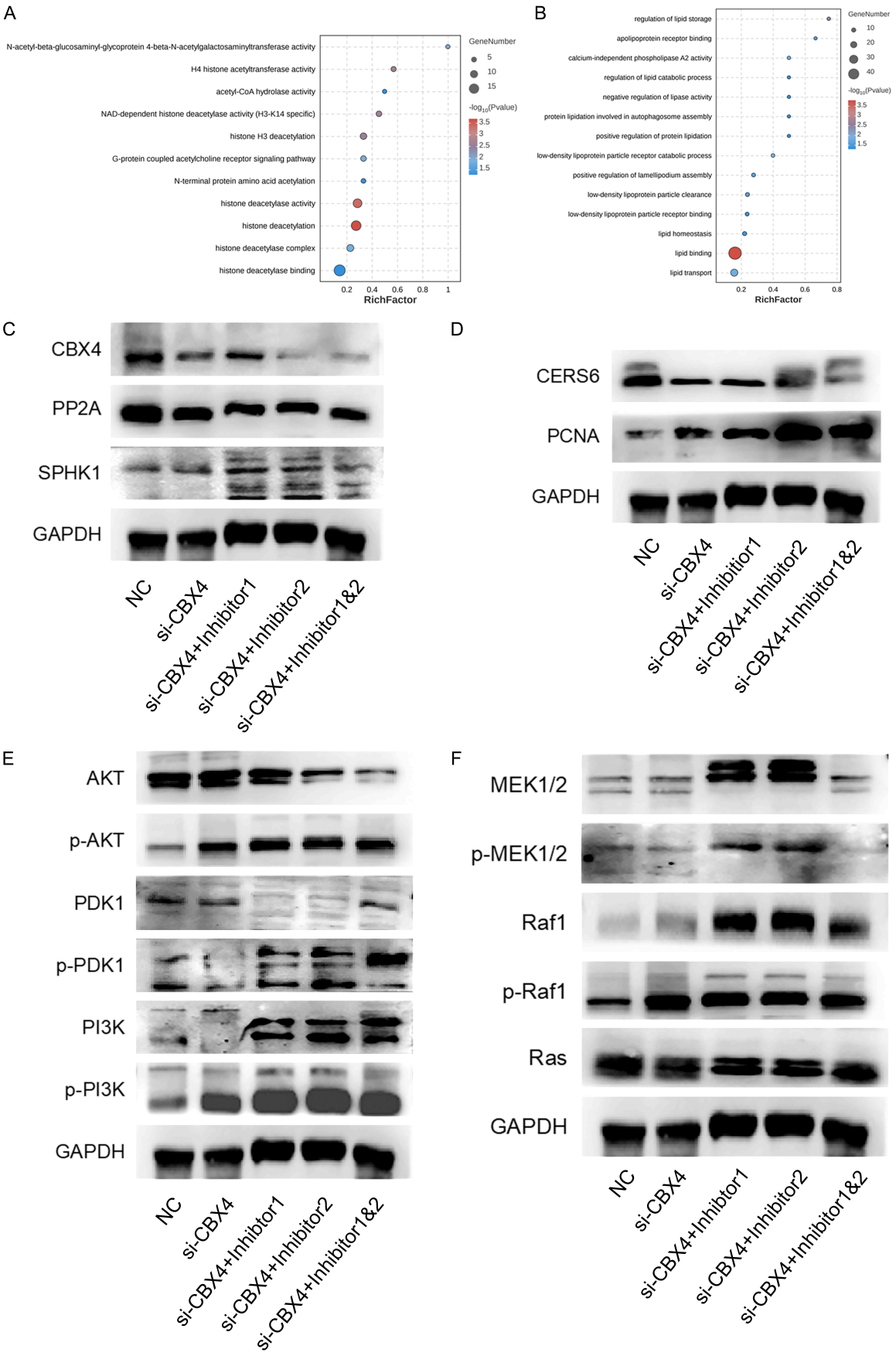
A
N-acetyl-beta-glucosaminyl-glycoprotein 4-beta-N-acetylgalactosaminyltransferase activity
H4 histone acetyltransferase activity
acetyl-CoA hydrolase activity
NAD-dependent histone deacetylase activity (H3-K14 specific)
histone H3 deacetylation
G-protein coupled acetylcholine receptor signaling pathway
N-terminal protein amino acid acetylation
histone deacetylase activity
histone deacetylation
histone deacetylase complex
histone deacetylase binding
GeneNumber
5
10
15
-log10(Pvalue)
3.5
3
2.5
2
1.5
0.2
0.4
0.6
0.8
1
RichFactor
B
regulation of lipid storage
apolipoprotein receptor binding
calcium-independent phospholipase A2 activity
regulation of lipid catabolic process
negative regulation of lipase activity
protein lipidation involved in autophagosome assembly
positive regulation of protein lipidation
low-density lipoprotein particle receptor catabolic process
positive regulation of lamellipodium assembly
low-density lipoprotein particle clearance
low-density lipoprotein particle receptor binding
lipid homeostasis
lipid binding
lipid transport
GeneNumber
10
20
30
40
-log10(Pvalue)
3.5
3
2.5
2
1.5
0.2
0.4
0.6
0.8
RichFactor
C
CBX4
PP2A
SPHK1
GAPDH
NC
si-CBX4
si-CBX4+Inhibitor1
si-CBX4+Inhibitor2
si-CBX4+Inhibitor1&2
D
CERS6
PCNA
GAPDH
NC
si-CBX4
si-CBX4+Inhibitior1
si-CBX4+Inhibitor2
si-CBX4+Inhibitor1&2
E
AKT
p-AKT
PDK1
p-PDK1
PI3K
p-PI3K
GAPDH
NC
si-CBX4
si-CBX4+Inhibtor1
si-CBX4+Inhibitor2
si-CBX4+Inhibitor1&2
F
MEK1/2
p-MEK1/2
Raf1
p-Raf1
Ras
GAPDH
NC
si-CBX4
si-CBX4+Inhibtor1
si-CBX4+Inhibitor2
si-CBX4+Inhibitor1&2

Figure 10. The role of CBX4 in ceramide regulation. Note: (A, B) KEGG pathway analysis of CBX4 involvement in acetylation and lipid metabolic signaling pathways. (C) Effect of its inhibitor on the expression of key proteins in SP metabolism. (D) Inhibitor effect on key proteins for SP metabolism. (E) Effect of the inhibitor on the expression of key proteins in disease progression. (F) Inhibitor effect on key proteins in disease progression.

taining intracellular SP homeostasis, particularly normal ceramide levels. In terms of cell proliferation regulation, si-CBX4 caused a significant decrease in the expression of its key downstream effector molecule, CERS6, which in turn promoted cell proliferation and altered the cell cycle progression [30]. When CERS6 was overexpressed in the context of CBX4 knockdown, the pro-proliferative phenotype induced by CBX4 deficiency was partially reversed, strongly demonstrating that CERS6 serves as a core downstream mediator through which CBX4 regulates cell proliferation [31]. Proteomic and mutant verification results elucidated the potential reasons for the above phenomena at the molecular level. By constructing a truncated mutant of CBX4, the study found that the deletion of its SUMO E3 ligase activity domain led to a significant upregulation of SUMO1 modification and CERS6 protein expression, accompanied by a decrease in H3K27me3 levels [32]. This key finding suggests that CBX4 likely regulates the protein stability and expression level of CERS6 through its SUMOylation-dependent post-tranlational modification and the repressive histone modification state maintained by the PRC1 complex, thereby influencing the entire sphingolipid metabolic network [33]. This indicates that the core mechanism by which CBX4 regulates SP metabolism is as follows: CBX4, through its protein modification functions and potential epigenetic regulation, inhibits HDAC5 expression, thereby alleviating HDAC5-mediated transcriptional repression of the CERS6 gene promoter, and ultimately maintaining CERS6 expression and ceramide synthesis. When CBX4 is knocked down (si-CBX4), this repressive regulation is lifted, leading to upregulation of HDAC5, suppression of CERS6 expression, and reduction of ceramide synthesis [34, 35]. Consequently, SP metabolic balance is disrupted, and pro-survival and pro-proliferative signaling pathways such as PI3K/AKT and MAPK are activated, collectively driving the malignant progression of AML.

To further validate the targeting relationships of CBX4, CUT&Tag and Co-IP experiments directly confirmed that CBX4 can bind to both CERS6 and HDAC5, establishing interactions between them. Importantly, the key regulatory hierarchy is reflected in the transcriptional repression of HDAC5 by CBX4 [36]. Knockdown of CBX4 led to a significant upregulation of HDAC5 mRNA and protein levels, whereas CBX4 overexpression had the opposite effect, indicating that CBX4 is an upstream transcriptional repressor of HDAC5. This relationship was further supported by dual-luciferase reporter gene assays, which confirmed that CBX4 suppressed the promoter activity of HDAC5 [37]. Co-IP experiments further verified the interaction between HDAC5 and CERS6, and knockdown of HDAC5 resulted in upregulated CERS6 protein expression. Mechanistically, HDAC5 directly acts on the CERS6 promoter and inhibits its transcriptional activity [38]. This clearly outlines a regulatory pathway: CBX4, by repressing HDAC5 expression, alleviates the transcriptional repression of the CERS6 promoter by HDAC5, ultimately maintaining CERS6 expression and ceramide synthesis [39, 40]. When CBX4 knockdown was combined with ceramide synthesis inhibitors, it synergistically enhanced the activation of the PI3K/AKT and MAPK signaling pathways. The potential mechanism behind this phenomenon is that CBX4 knockdown and pharmacological inhibition work together to exacerbate the depletion of intracellular ceramide [41]. As a known tumor-suppressive lipid molecule, decreased ceramide levels release the brake on pro-survival signaling pathways, thereby strongly activating the AKT and MEK/ERK pathways and driving malignant cell proliferation [42]. This explains why targeted intervention of this axis could represent an effective therapeutic strategy [43]. In summary, these findings reveal a sophisticated cascade regulatory model in AML: CBX4 acts as an upstream regulatory factor that indirectly promotes CERS6 expression and ceramide synthesis by transcriptionally repressing HDAC5, thereby helping to maintain a relative metabolic balance and suppress excessive proliferative signaling [44]. When CBX4 function is lost, this balance is disrupted. Upregulated HDAC5 subsequently represses CERS6 transcription, lead-

ing to decreased ceramide levels [45]. Ultimately, by relieving the inhibition on the PI3K/AKT and MAPK pathways, this process vigorously promotes the malignant progression of leukemia.

While this study elucidates the regulatory role of the CBX4-HDAC5-CERS6 axis in SP metabolism in AML, several limitations should be noted. First, this study primarily relies on *in vitro* cell line models and lacks validation through *in vivo* animal experiments. Subsequent animal studies are still needed to evaluate the function of this axis within the complex tumor microenvironment, its impact on leukemogenesis and progression, and potential systemic toxicity. Second, the precise epigenetic mechanisms by which HDAC5 suppresses CERS6 transcription have not been fully elucidated. The indirect pathway through which CBX4 regulates HDAC5 expression also requires further clarification.

Conclusion

Aberrant CBX4 expression alters SP metabolism in AML by modulating HDAC5-mediated repression on CERS6. Reduced CBX4 expression attenuates the inhibitory effect on HDAC5, leading to HDAC5 upregulation and enhanced repression of CERS6 transcription. Consequently, CERS6 downregulation disrupts SP biosynthesis and compromises cellular membrane stability.

Acknowledgements

This work was supported by the National Natural Science Foundation of China (82073582 and 82103876), the Guangdong Basic and Applied Basic Research Foundation (2023A1515140169), the Guangdong Provincial University Key Platform Featured Innovation Project (2020KTSCX048), and the Discipline Construction Project from Guangdong Medical University (4SG23003G).

Disclosure of conflict of interest

None.

Address correspondence to: Huanwen Tang, School of Public Health, The Affiliated Dongguan Occupational Disease Prevention and Control Hospital, Guangdong Medical University, Dongguan, Guangdong, China. E-mail: thw@gdmu.edu.cn

References

[1] Dembitz V, James SC and Gallipoli P. Targeting lipid metabolism in acute myeloid leukemia: biological insights and therapeutic opportunities. Leukemia 2025; 39: 1814-1823.
[2] Schrezenmeier J and Huntly BJP. Epigenetic dysregulation in acute myeloid leukemia. Semin Hematol 2025; 62: 177-186.
[3] Xiao H, Hu X, Li P and Deng J. Global burden and trends of leukemia attributable to high body mass index risk in adults over the past 30 years. Front Oncol 2024; 14: 1404135.
[4] Singh P, Murali R, Shanmugam SG, Thomas S, Scott J, Warrier S, Arfuso F, Dharmarajan A and Gandhirajan RK. Aberrant lipid metabolic signatures in acute myeloid leukemia. Stem Cells 2024; 42: 200-215.
[5] Ung J, Tan SF, Fox TE, Shaw JJP, Vass LR, Costa-Pinheiro P, Garrett-Bakelman FE, Keng MK, Sharma A, Claxton DF, Levine RL, Tallman MS, Cabot MC, Kester M, Feith DJ and Loughran TP Jr. Harnessing the power of sphingolipids: prospects for acute myeloid leukemia. Blood Rev 2022; 55: 100950.
[6] Quinville BM, Deschenes NM, Ryckman AE and Walia JS. A comprehensive review: sphingolipid metabolism and implications of disruption in sphingolipid homeostasis. Int J Mol Sci 2021; 22: 5793.
[7] Takehara M, Bandou H, Kobayashi K and Nagahama M. Clostridium perfringens α-toxin specifically induces endothelial cell death by promoting ceramide-mediated apoptosis. Anaerobe 2020; 65: 102262.
[8] O'Brien C and Jones CL. Unraveling lipid metabolism for acute myeloid leukemia therapy. Curr Opin Hematol 2025; 32: 77-86.
[9] Pitman MR, Lewis AC, Davies LT, Moretti PAB, Anderson D, Creek DJ, Powell JA and Pitson SM. The sphingosine 1-phosphate receptor 2/4 antagonist JTE-013 elicits off-target effects on sphingolipid metabolism. Sci Rep 2022; 12: 454.
[10] Zhao Z, Xu S, Ma J, Zhang Z, Liang S and Guo J. Macrophage CBX4 potentiates atherosclerosis by its SUMO E3 ligase activity. Cardiovasc Drugs Ther 2025; [Epub ahead of print].
[11] Li H, Xu Y, Zheng Y, Xue Z, Li Q, Jia X, Weng L, Jiang L, Ruan X, Zhang R, Yin Y, Zhou L, Li F, Huang H, Li J, Tan M, Fan J, Cai J, Chen G and Zhou L. CBX4 acetoacetylation as an inhibitory mechanism of HIF-1α activity. Cell Chem Biol 2025; 32: 1249-1259, e9.
[12] Huang W, Yu C, Wu H, Liang S, Kang J, Zhou Z, Liu A and Liu L. Cbx4 governs HIF-1α to involve in Th9 cell differentiation promoting asthma by its SUMO E3 ligase activity. Biochim Biophys Acta Mol Cell Res 2023; 1870: 119524.

[13] Chang MM, Hong YK, Hsu CK, Harn HI, Huang BM, Liu YH, Lu FI, Hsueh YY, Lin SP and Wu CC. Histone Trimethylations and HDAC5 regulate spheroid subpopulation and differentiation signaling of human adipose-derived stem cells. Stem Cells Transl Med 2024; 13: 293-308.

[14] Jiang N, Niu G, Pan YH, Pan W, Zhang MF, Zhang CZ and Shen H. CBX4 transcriptionally suppresses KLF6 via interaction with HDAC1 to exert oncogenic activities in clear cell renal cell carcinoma. EBioMedicine 2020; 53: 102692.

[15] Zhu Z, Cao Y, Jian Y, Hu H, Yang Q, Hao Y, Jiang H, Luo Z, Yang X, Li W, Hu J, Liu H, Liang W, Ding G and Chen Z. CerS6 links ceramide metabolism to innate immune responses in diabetic kidney disease. Nat Commun 2025; 16: 1528.

[16] Xu A, Liu Y, Wang B, Zhang Q, Ma Y, Xue Y, Wang Z, Sun Q, Sun Y and Bian L. Ceramide synthase 6 induces mitochondrial dysfunction and apoptosis in hemin-treated neurons by impairing mitophagy through interacting with sequestosome 1. Free Radic Biol Med 2025; 227: 282-295.

[17] Suzuki M, Cao K, Kato S, Mizutani N, Tanaka K, Arima C, Tai MC, Nakatani N, Yanagisawa K, Takeuchi T, Shi H, Mizutani Y, Niimi A, Taniguchi T, Fukui T, Yokoi K, Wakahara K, Hasegawa Y, Mizutani Y, Iwaki S, Fujii S, Satou A, Tamiya-Koizumi K, Murate T, Kyogashima M, Tomida S and Takahashi T. CERS6 required for cell migration and metastasis in lung cancer. J Cell Mol Med 2020; 24: 11949-11959.

[18] Wegner MS, Gruber L, Schömel N, Trautmann S, Brachtendorf S, Fuhrmann D, Schreiber Y, Olesch C, Brüne B, Geisslinger G and Grösch S. GPER1 influences cellular homeostasis and cytostatic drug resistance via influencing long chain ceramide synthesis in breast cancer cells. Int J Biochem Cell Biol 2019; 112: 95-106.

[19] Pollyea DA, Bixby D, Perl A, Bhatt VR, Altman JK, Appelbaum FR, de Lima M, Fathi AT, Foran JM, Gojo I, Hall AC, Jacoby M, Lancet J, Mannis G, Marcucci G, Martin MG, Mims A, Neff J, Nejati R, Olin R, Percival ME, Prebet T, Przespolewski A, Rao D, Ravandi-Kashani F, Shami PJ, Stone RM, Strickland SA, Sweet K, Vachhani P, Wieduwilt M, Gregory KM, Ogba N and Tallman MS. NCCN guidelines insights: acute myeloid leukemia, version 2.2021. J Natl Compr Canc Netw 2021; 19: 16-27.

[20] Song GY, Kim HJ, Kim T, Ahn SY, Jung SH, Kim M, Yang DH, Lee JJ, Kim MY, Cheong JW, Jung CW, Jang JH, Kim HJ, Moon JH, Sohn SK, Won JH, Park SK, Kim SH, Choi CK, Kim HJ, Ahn JS and Kim DDH. Validation of the 2022 European LeukemiaNet risk stratification for acute myeloid leukemia. Sci Rep 2024; 14: 8517.

[21] Versluis J, Pandey M, Flamand Y, Haydu JE, Belizaire R, Faber M, Vedula RS, Charles A, Copson KM, Shimony S, Rozental A, Bendapudi PK, Wolach O, Griffiths EA, Thompson JE, Stone RM, DeAngelo DJ, Neuberg D, Luskin MR, Wang ES and Lindsley RC. Prediction of life-threatening and disabling bleeding in patients with AML receiving intensive induction chemotherapy. Blood Adv 2022; 6: 2835-2846.

[22] Ito H, Nakamae I, Kato JY and Yoneda-Kato N. Stabilization of fatty acid synthesis enzyme acetyl-CoA carboxylase 1 suppresses acute myeloid leukemia development. J Clin Invest 2021; 131: e141529.

[23] Mohanty V, Baran N, Huang Y, Ramage CL, Cooper L, Pelletier SG, He S, Iqbal R, Daher M and Tyner JW. Elucidating transcriptional heterogeneity in venetoclax resistant AMLs. Blood 2024; 144: 2753.

[24] Stevens BM, Jones CL, Pollyea DA, Culp-Hill R, D'Alessandro A, Winters A, Krug A, Abbott D, Goosman M, Pei S, Ye H, Gillen AE, Becker MW, Savona MR, Smith C and Jordan CT. Fatty acid metabolism underlies venetoclax resistance in acute myeloid leukemia stem cells. Nat Cancer 2020; 1: 1176-1187.

[25] Bazinet A and Kantarjian HM. Moving toward individualized target-based therapies in acute myeloid leukemia. Ann Oncol 2023; 34: 141-151.

[26] Lo Presti C, Yamaryo-Botté Y, Mondet J, Berthier S, Nutiu D, Botté C and Mossuz P. Variation in lipid species profiles among leukemic cells significantly impacts their sensitivity to the drug targeting of lipid metabolism and the prognosis of AML patients. Int J Mol Sci 2023; 24: 5988.

[27] Zhang J, Liu Y, Yin W and Hu X. Adipose-derived stromal cells in regulation of hematopoiesis. Cell Mol Biol Lett 2020; 25: 16.

[28] Bao G, Huang J, Pan W, Li X and Zhou T. Long noncoding RNA CERS6-AS1 functions as a malignancy promoter in breast cancer by binding to IGF2BP3 to enhance the stability of CERS6 mRNA. Cancer Med 2020; 9: 278-289.

[29] Uen YH, Fang CL, Lin CC, Hseu YC, Hung ST, Sun DP and Lin KY. Ceramide synthase 6 predicts the prognosis of human gastric cancer: it functions as an oncoprotein by dysregulating the SOCS2/JAK2/STAT3 pathway. Mol Carcinog 2018; 57: 1675-1689.

[30] Shi H, Niimi A, Takeuchi T, Shiogama K, Mizutani Y, Kajino T, Inada K, Hase T, Hatta T, Shibata H, Fukui T, Chen-Yoshikawa TF, Nagano K, Murate T, Kawamoto Y, Tomida S, Takahashi T and Suzuki M. CEBPγ facilitates lamellipodia formation and cancer cell migration through

CERS6 upregulation. Cancer Sci 2021; 112: 2770-2780.
[31] Al-Rashed F, Ahmad Z, Snider AJ, Thomas R, Kochumon S, Melhem M, Sindhu S, Obeid LM, Al-Mulla F, Hannun YA and Ahmad R. Ceramide kinase regulates TNF-α-induced immune responses in human monocytic cells. Sci Rep 2021; 11: 8259.
[32] Tang S, Liang C, Yu H, Hou W, Hu Z, Chen X, Duan Z and Zheng S. The potential serum sphingolipid biomarkers for distinguishing Wilson disease. Clin Chim Acta 2024; 553: 117740.
[33] Wang X, Li L, Wu Y, Zhang R, Zhang M, Liao D, Wang G, Qin G, Xu RH and Kang T. CBX4 suppresses metastasis via recruitment of HDAC3 to the Runx2 promoter in colorectal carcinoma. Cancer Res 2016; 76: 7277-7289.
[34] Chen Q, Huang L, Pan D, Zhu LJ and Wang YX. Cbx4 sumoylates Prdm16 to regulate adipose tissue thermogenesis. Cell Rep 2018; 22: 2860-2872.
[35] Yan X, Kang D, Lin Y, Qi S and Jiang C. CBX4-dependent regulation of HDAC3 nuclear translocation reduces Bmp2-induced osteoblastic differentiation and calcification in adamantinomatous craniopharyngioma. Cell Commun Signal 2022; 20: 3.
[36] Yang J, Gong C, Ke Q, Fang Z, Chen X, Ye M and Xu X. Insights into the function and clinical application of HDAC5 in cancer management. Front Oncol 2021; 11: 661620.
[37] Zhou Y, Jin X, Ma J, Ding D, Huang Z, Sheng H, Yan Y, Pan Y, Wei T, Wang L, Wu H and Huang H. HDAC5 loss impairs RB repression of prooncogenic genes and confers CDK4/6 inhibitor resistance in cancer. Cancer Res 2021; 81: 1486-1499.
[38] Wang J, Wu S, Liu L, Pang Y, Li Z and Mu H. HDAC5-mediated acetylation of p100 suppresses its processing. Int Dent J 2023; 73: 387-394.
[39] Ramaiah MJ, Tangutur AD and Manyam RR. Epigenetic modulation and understanding of HDAC inhibitors in cancer therapy. Life Sci 2021; 277: 119504.
[40] Olaniyi KS, Amusa OA, Ajadi IO, Alabi BY, Agunbiade TB and Ajadi MB. Repression of HDAC5 by acetate restores hypothalamic-pituitary-ovarian function in type 2 diabetes mellitus. Reprod Toxicol 2021; 106: 69-81.
[41] Yi Q, Huang M, Zhang X, Xu Z, Sun J, Wang S, Xu H, Du Z and Liu M. GNA13 inhibits glioblastoma metastasis via the ERKs/FOX03 signaling pathway. Cell Signal 2023; 109: 110789.
[42] van den Bos E, Ambrosy B, Horsthemke M, Walbaum S, Bachg AC, Wettschureck N, Innamorati G, Wilkie TM and Hanley PJ. Knockout mouse models reveal the contributions of G protein subunits to complement C5a receptor-mediated chemotaxis. J Biol Chem 2020; 295: 7726-7742.
[43] Ji J, Yin Y, Ju H, Xu X, Liu W, Fu Q, Hu J, Zhang X and Sun B. Long non-coding RNA Lnc-Tim3 exacerbates CD8 T cell exhaustion via binding to Tim-3 and inducing nuclear translocation of Bat3 in HCC. Cell Death Dis 2018; 9: 478.
[44] Wang J, Jia W, Zhou X, Ma Z, Liu J and Lan P. CBX4 suppresses CD8(+) T cell antitumor immunity by reprogramming glycolytic metabolism. Theranostics 2024; 14: 3793-3809.
[45] Liu Z, Liu Y, Fu Z, Huang H, Wang R, Wang Z, Peng S, Wang J, Fang Z and Liu L. Integrating single-cell and bulk RNA sequencing reveals the malignant phenotype of CBX4 in prostate cancer. J Cancer 2025; 16: 3525-3536.